



# Thermal stability of artinite, dypingite and brugnatellite—Implications for the geosequestration of green house gases

Ray L. Frost\*, Silmarilly Bahfenne, Jessica Graham, Wayne N. Martens

*Inorganic Materials Research Program, School of Physical and Chemical Sciences, Queensland University of Technology, GPO Box 2434, Brisbane, Queensland 4001, Australia*

## ARTICLE INFO

### Article history:

Received 7 April 2008

Received in revised form 22 June 2008

Accepted 24 June 2008

Available online 4 July 2008

### Keywords:

Artinite

Dypingite

Brugnatellite

Carbonate

Thermal stability

Thermogravimetry

Thermal analysis

Geological sequestration of CO<sub>2</sub>

## ABSTRACT

The approach to remove green house gases by pumping liquefied carbon dioxide several kilometres below the ground implies that many carbonate containing minerals will be formed. Among these minerals the formation of dypingite, artinite and if the ferric iron is present brugnatellite are possible; thus necessitating a study of the thermal stability of such minerals. The thermal stability of two carbonate bearing minerals dypingite and artinite together with brugnatellite with a hydrotalcite related formulae have been characterised by a combination of thermogravimetry and evolved gas mass spectrometry. Artinite is thermally stable up to 352 °C. Two mass loss steps are observed at 219 and 355 °C. Dypingite decomposes at a similar temperature but over a large number of steps. Brugnatellite shows greater stability with decomposition not occurring until after 577 °C. The thermal decomposition of brugnatellite occurs over a number of mass decomposition steps. It is concluded that pumping liquefied green house gases into magnesium bearing mineral deposits is feasible providing a temperature of 350–355 °C is not exceeded to prevent escape of CO<sub>2</sub> towards the surface. In contrast, the water loss occurring at lower temperatures could have a positive effect on the geosequestration of CO<sub>2</sub> as it probably causes a decrease in the molar volume of secondary carbonate minerals and consequently an increase in aquifer porosity.

© 2008 Elsevier B.V. All rights reserved.

## 1. Introduction

The ability to be able to easily and readily detect minerals is of importance [1,2]. This is especially so where carbonate minerals are concerned. What is probably not appreciated is that many carbonate containing minerals especially the secondary minerals are soluble and can be decomposed upon heating. The proposal to remove green house gases by pumping liquid-like CO<sub>2</sub> in deep aquifers (>800 m approx.), chiefly hosted in sedimentary basins, is expected to cause formation of many carbonate containing minerals [3–6]. Two magnesium carbonate minerals which may form under such conditions of high CO<sub>2</sub> partial pressure are dypingite Mg<sub>5</sub>(CO<sub>3</sub>)<sub>4</sub>(OH)<sub>2</sub>·5H<sub>2</sub>O [7–11] and artinite Mg<sub>2</sub>(CO<sub>3</sub>)(OH)<sub>2</sub>·3H<sub>2</sub>O [12–21]. Other magnesium containing minerals are the ferric ion bearing minerals coalingite Mg<sub>10</sub>Fe<sub>2</sub><sup>3+</sup>(CO<sub>3</sub>)(OH)<sub>24</sub>·2(H<sub>2</sub>O), [22–29] and brugnatellite Mg<sub>6</sub>Fe<sup>3+</sup>(CO<sub>3</sub>)(OH)<sub>13</sub>·4(H<sub>2</sub>O) [27,30–34] and hydrotalcite Mg<sub>6</sub>Al<sub>2</sub>(CO<sub>3</sub>)(OH)<sub>16</sub>·4(H<sub>2</sub>O). The formulae of these first two minerals appear to be related to that of hydrotalcites. Pastor-Rodriguez and Taylor reported the crystal structure of coalingite and presented a model coalingite with a *d*(003) spacing of 1.25 nm [29].

Brugnatellite is related to the manasseite–pyroaurite mineral group [Mg<sub>6</sub>R<sub>2</sub><sup>3+</sup>(CO<sub>3</sub>)(OH)<sub>16</sub>·4(H<sub>2</sub>O), where R<sup>3+</sup> = Al, Cr or Fe].

The study of the magnesium carbonates is of extreme importance in the development of technology for the removal of green house gases. Magnesium minerals such as brucite, periclase and several Mg–silicates (e.g., the serpentine group minerals, forsterite, etc.) have the potential for the sequestration of carbon dioxide. Hydrotalcites may also be used but must be first thermally activated [35]. Studies of the thermodynamic [6] and phase diagrams [13] of related magnesium minerals have been published [36]. The reaction path involving carbonation of brucite (Mg(OH)<sub>2</sub>) is particularly complex, as Mg has a strong tendency to form a series of metastable hydrous carbonates. These metastable hydrous carbonates include hydromagnesite (Mg<sub>5</sub>(CO<sub>3</sub>)<sub>4</sub>(OH)<sub>2</sub>·4H<sub>2</sub>O, artinite (Mg<sub>2</sub>CO<sub>3</sub>(OH)<sub>2</sub>·3H<sub>2</sub>O), nesquehonite (MgCO<sub>3</sub>·3H<sub>2</sub>O), and lansfordite (MgCO<sub>3</sub>·5H<sub>2</sub>O). The free energy of formation for these hydroxy and hydrous carbonates differs and their generation depends on the partial pressure of CO<sub>2</sub> [6].

Thermal analysis using thermogravimetric techniques enables the mass loss steps, the temperature of the mass loss steps and the mechanism for the mass loss to be determined [37–43]. Thermoanalytical methods provide a measure of the thermal stability of the hydrotalcite and related minerals. Structural information on different minerals has successfully been obtained recently by sophisticated thermal analysis techniques [37–42]. In this work we

\* Corresponding author. Tel.: +61 7 3138 2407; fax: +61 7 3138 1804.  
E-mail address: [r.frost@qut.edu.au](mailto:r.frost@qut.edu.au) (R.L. Frost).

report the thermal analysis of the magnesium carbonate minerals artinite, dypingite and brugnatellite.

## 2. Experimental

### 2.1. Minerals

The following minerals were used in this research (a) Dypingite: Yoshikawaite, Shinshiro Shi, Aichi Prefecture, Japan, (b) Sample 4 Dypingite: Clear Creek District, Southern San Benito County, California, (c) Sample 3 Artinite: Clear Creek District, Southern San Benito County, California and (d) Sample 7 Artinite: Higasi-Kuroda-Guchi, Inasa-Cho, Inasa-Gun, Aichi Prefecture, Japan.

The origin of the brugnatellite minerals is as follows: (e) Brugnatellite: Monte, Ramazzo, Genoa, Liguria, Italy; (f) Brugnatellite: Higasi-Kuroda-Guchi, Inasa-Cho, Inasa-Gun, Aichi Prefecture, Japan. The minerals are associated with iron-containing brucite.

### 2.2. Thermal analysis

Thermal decomposition of the magnesium carbonates was carried out in a TA<sup>®</sup> Instruments incorporated high-resolution thermogravimetric analyzer (series Q500) in a flowing nitrogen atmosphere ( $60 \text{ cm}^3 \text{ min}^{-1}$ ). Approximately 35 mg of sample underwent thermal analysis, with a heating rate of  $5^\circ \text{C min}^{-1}$ , and high resolution, to  $1000^\circ \text{C}$ . With the heating program of the instrument the furnace temperature was regulated precisely to provide a uniform rate of decomposition in the main decomposition stage. The TGA instrument was coupled to a Balzers (Pfeiffer) mass spectrometer for gas analysis. Only water vapour, carbon dioxide and oxygen were analysed.

## 3. Results and discussion

In order to make a study of the potential of these carbonate minerals for geosequestration it is important to use the natural minerals. Thus, there may arise differences between the experimental mass losses and the theoretical mass losses, because of (a) impurities in the minerals and (b) partial dehydration. It is worthwhile noting that there have been detailed studies of artinite including the thermodynamic properties [44,45]. The comment may be also made that there have been no thermodynamic or detailed studies on dypingite and brugnatellite.

The thermogravimetric and differential thermogravimetric analysis of artinite  $\text{Mg}_2\text{CO}_3(\text{OH})_2 \cdot 3\text{H}_2\text{O}$  is shown in Fig. 1. The ion current curves for the evolved gas analysis are displayed in Fig. 2. Two mass loss steps at 219 and  $352^\circ \text{C}$  with mass losses of 26 and 24% are observed. The following reactions are proposed for the

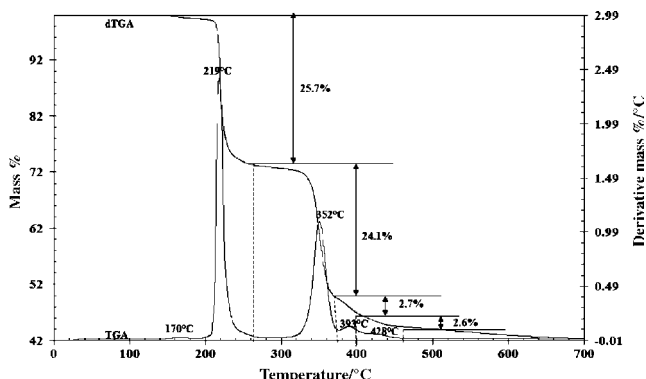


Fig. 1. Thermal analysis and differential thermal analysis of artinite.

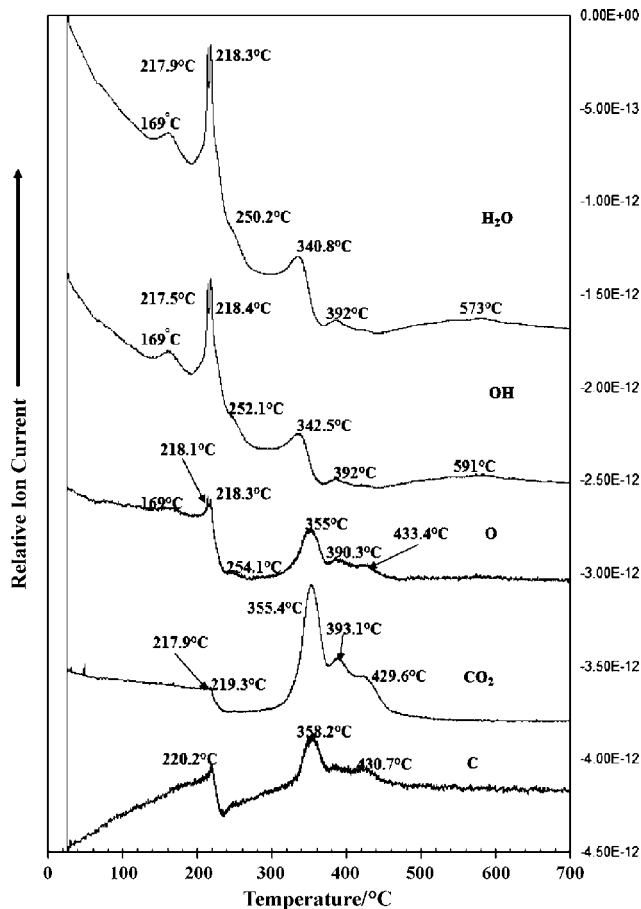
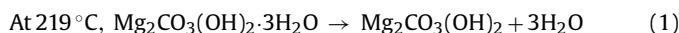


Fig. 2. Ion current curves for the gas evolution during the decomposition of artinite.

thermal decomposition of artinite:



The thermogravimetric and differential thermogravimetric analysis for artinite clearly shows that water is lost at  $219^\circ \text{C}$ . The ion current curves suggest water is lost at 169, 218 and  $218^\circ \text{C}$ . Some water vapour is measured at  $341^\circ \text{C}$ . The ion current curves prove that  $\text{CO}_2$  is evolved at 355, 393 and  $429^\circ \text{C}$ . The theoretical mass loss for the first reaction, the dehydration step is 27%. The observed mass loss of 26% is comparable. It is proposed in reaction (2) that decarbonation and dehydroxylation take place simultaneously. The theoretical mass loss for dehydroxylation is 8.67% and for decarbonation is 22%. Thus the theoretical mass loss is  $\sim 31\%$ . The observed mass loss at  $352^\circ \text{C}$  is 24%. Two small mass losses at 393 and  $428^\circ \text{C}$  of 2.7 and 2.6% are observed. The total observed mass loss over the 300 to  $500^\circ \text{C}$  is 29% which is comparable with the calculated expected mass loss.

References to previous studies on the thermal decomposition of artinite are very few. Beck [46] reported the DTA patterns of artinite. In the DTA, Beck reported the decomposition to start at  $230^\circ \text{C}$  with the loss of 'water of crystallisation' with a maximum at  $280^\circ \text{C}$ . Dehydroxylation was found to occur at  $385^\circ \text{C}$  and decarbonation at  $540^\circ \text{C}$ . The DTA pattern reported by Beck (p. 1001) shows strong asymmetry and may indicate a rapid heating rate which has skewed the DTA patterns. This result in the displacement of the temperatures of the thermal decomposition to higher temperatures than might be found if the heating rate was significantly less. The observation by Beck that the dehydroxylation occurs at  $280^\circ \text{C}$  fits

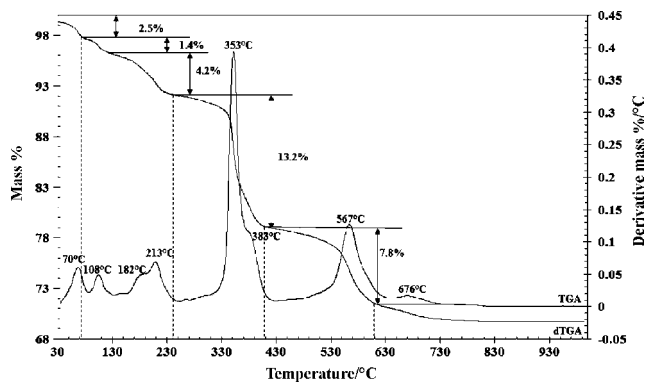


Fig. 3. Thermal analysis and differential thermal analysis of dypingite.

reasonably well with the dehydration temperature of 219 °C. Beck also indicated that dehydroxylation and decarbonation overlapped. This observation fits well with the DTG peak at 352 °C.

The thermal decomposition of dypingite  $Mg_5(CO_3)_4(OH)_2 \cdot 5H_2O$  is reported in Fig. 3. The ion current curves for the evolved gases from the dypingite sample are reported in Fig. 4. Four mass loss steps at 70, 108, 182 and 213 °C are observed with a total mass loss of 8%. This value is less than the calculated value of 18%. This difference is attributed to the presence of other minerals in the dypingite mineral sample. The observation of four mass loss steps suggests the water is lost in steps. The ion current curves for dypingite show that

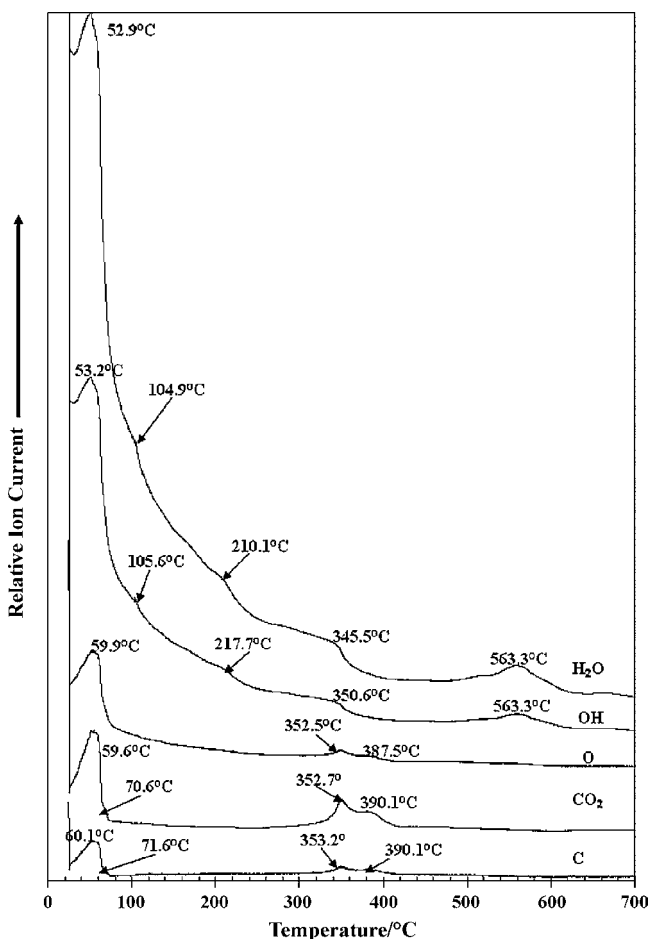


Fig. 4. Ion current curves for the gas evolution during the decomposition of dypingite.

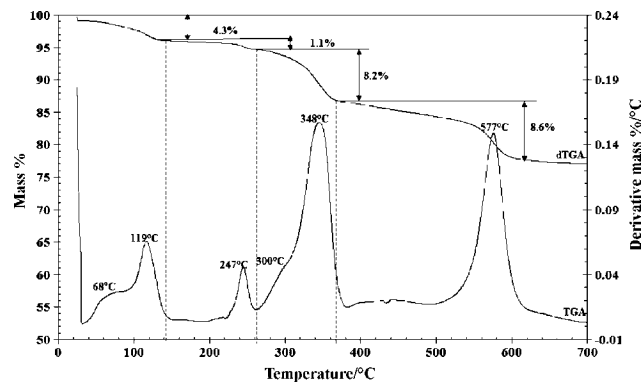


Fig. 5. Thermal analysis and differential thermal analysis of brugnatellite.

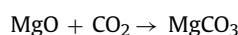
water is lost at 53, 105, 210 and 346 °C, thus confirming that water is lost in stages. It is possible that water is lost as high as 353 °C. Two mass decomposition steps at 353 and 388 °C are observed and are attributed to partial dehydration and dehydroxylation. The mass loss at 567 °C is assigned to the decarbonation and partial dehydroxylation of the dypingite. The calculated mass loss is 10% which is close to the observed value of 8%. To the best of the authors' knowledge there have been few reported thermal analyses of dypingite as compared with some other magnesium carbonate minerals [8,10].

The thermal analysis of the mineral brugnatellite  $Mg_6Fe^{3+}(CO_3)(OH)_{13} \cdot 4H_2O$  is shown in Fig. 5. The ion current curves are reported in Fig. 6. The ion current curves for  $H_2O$  shows that water is evolved at 67, 118, 245, 297, 349 and 579 °C. The ion current curves for  $CO_2$  show that this gas is evolved at predominantly 336, 354 and 422 °C. This latter peak maximum is broad and covers a wide temperature range. This shows that the decomposition of the brugnatellite takes place over a wide temperature range. Thermally induced mass loss steps are observed at 68, 119, 247, 300, 348 and 577 °C. The first two mass loss steps are ascribed to dehydration with a mass loss of 4% which cannot be compared with the calculated value of 13%. The mass loss at 247 °C is a dehydroxylation step. The mass loss at 348 °C attributed to a combination of decarbonation and dehydroxylation is 8%. The mass loss at 577 °C is 8.6% and is assigned based upon the ion current curves to decarbonation. The mass loss of  $CO_2$  at 577 °C is 9% as compared with the calculated value of 8% based upon the formula  $Mg_6Fe^{3+}(CO_3)(OH)_{13} \cdot 4H_2O$ . It is concluded that dehydration, dehydroxylation, and decarbonation are occurring over several temperature ranges and there is no clear peak that can be assigned to any of these processes.

### 3.1. Possible chemical reactions

In order to understand the potential chemical reactions of green house gases through reaction with magnesium minerals, it is important to set up model reactions and to understand these reactions. In this work, we have used the reaction of  $CO_2$  with brucite and periclase as model reactions. In reality reaction of  $CO_2$  with many compounds of Mg including silicates will need to be studied. It is important to have fundamental knowledge of the reactions of  $Mg(OH)_2$  and  $MgO$  with  $CO_2$  [36,47]. It is important to understand that the conditions of the reaction will affect the products in the following reactions [36]. Botha and Strydom showed that the reaction conditions including slurry pH, slurry temperature, drying temperature, drying time influence the product formation [36].

The following reactions may be envisaged:



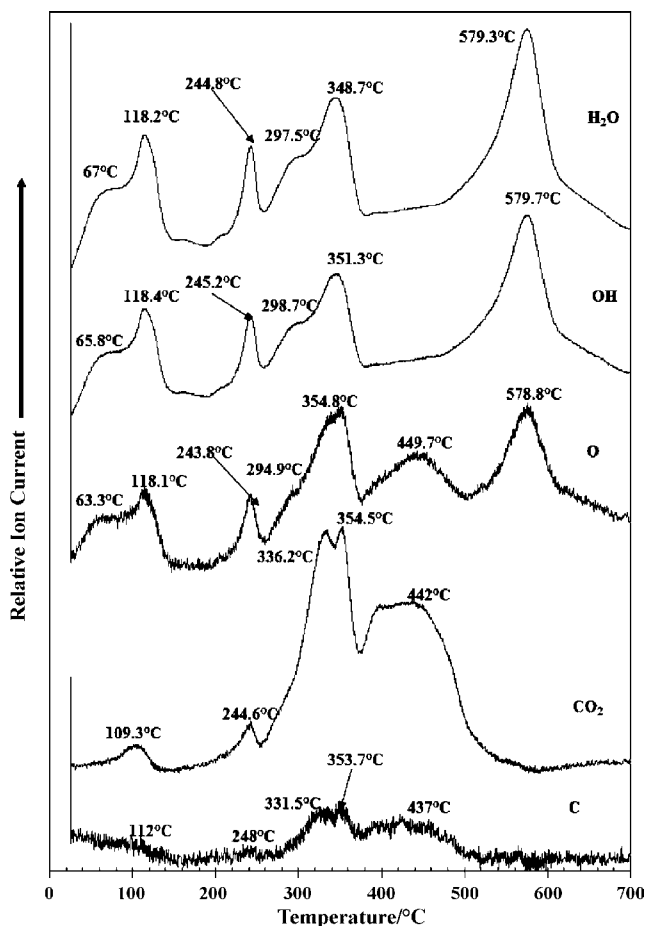
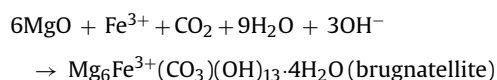
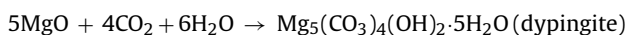


Fig. 6. Ion current curves for the gas evolution during the decomposition of brugnatellite.

and



It is important to understand the stability of such minerals both in terms of temperature and partial pressure of the  $\text{CO}_2$  [13]. The hydration–carbonation or hydration–and–carbonation reaction path in the  $\text{CO}_2$ – $\text{MgO}$ – $\text{H}_2\text{O}$  system at ambient temperature and atmospheric  $\text{CO}_2$  is of practical significance from the standpoint of carbon balance and the removal of green house gases from the atmosphere. A better understanding of the global masses of Mg and  $\text{CO}_2$  and the thermal stability of the hydrated carbonates of magnesium provide a practical understanding for carbon dioxide removal. From a practical point of view, the exact knowledge of the reaction path in  $\text{MgO}$ – $\text{CO}_2$ – $\text{H}_2\text{O}$  system is of great significance to the performance of  $\text{Mg}(\text{OH})_2$  and related minerals for green house gas removal. The reaction path involving carbonation of brucite ( $\text{Mg}(\text{OH})_2$ ) is particularly complex, as Mg has a strong tendency to form a series of metastable hydrous carbonates. These metastable hydrous carbonates include hydromagnesite ( $\text{Mg}_5(\text{CO}_3)_4(\text{OH})_2 \cdot 4\text{H}_2\text{O}$ , or  $\text{Mg}_4(\text{CO}_3)_3(\text{OH})_2 \cdot 3\text{H}_2\text{O}$ ), artinite ( $\text{Mg}_2\text{CO}_3(\text{OH})_2 \cdot 3\text{H}_2\text{O}$ ), dypingite  $\text{Mg}_5(\text{CO}_3)_4(\text{OH})_2 \cdot 5\text{H}_2\text{O}$ ,

nesquehonite ( $\text{MgCO}_3 \cdot 3\text{H}_2\text{O}$ ), and lansfordite ( $\text{MgCO}_3 \cdot 5\text{H}_2\text{O}$ ) and if  $\text{Fe}^{3+}$  is present and available then minerals such as brugnatellite and coalingite may be formed. The free energy of formation for these hydroxy and hydrous carbonates differs and their formation will depend on the partial pressure of  $\text{CO}_2$ .

#### 4. Conclusions

The potential for using magnesium ore deposits for the geosequestration of green house gases is real. Such a system will depend at least in part on the formation of a range of magnesium carbonate minerals including artinite, dypingite and brugnatellite. This work has shown that dehydration of these minerals occurs at  $219^\circ\text{C}$  for artinite,  $213^\circ\text{C}$  for dypingite and  $247^\circ\text{C}$  for brugnatellite, whereas decarbonation takes place at  $350$ – $355^\circ\text{C}$  for the three magnesium hydroxyl–carbonate minerals. Water loss and  $\text{CO}_2$  loss from these solid phases upon heating have different impact on the geosequestration of  $\text{CO}_2$  through injection of liquid-like  $\text{CO}_2$  in deep aquifers, chiefly hosted in sedimentary basins. The first process (water loss) could have a positive effect as it probably causes a decrease in the molar volume of secondary hydroxyl–carbonate minerals and consequently an increase in aquifer porosity, whereas the second process ( $\text{CO}_2$  loss) has a negative effect (owing to the possible escape of the  $\text{CO}_2$  towards the surface) and must absolutely be avoided.

#### Acknowledgments

The financial and infra-structure support of the Queensland University of Technology, Inorganic Materials Research Program is gratefully acknowledged. The Australian Research Council (ARC) is thanked for funding the instrumentation.

#### References

- [1] G.R. Hunt, R.P. Ashley, *Econ. Geol. Bull. Soc. Econ. Geol.* 74 (1979) 1613–1629.
- [2] G.R. Hunt, R.C. Everts, *Geophysics* 46 (1981) 316–321.
- [3] J.W. Anthony, R.A. Bideaux, K.W. Bladh, M.C. Nichols, *Handbook of Mineralogy*, Mineral Data Publishing, Tucson, Arizona, USA, 2003.
- [4] L.B. Railsback, *Carbonates Evaporites* 14 (1999) 1–20.
- [5] S.W.M. Blake, C. Cuff, *Preparation and Use of Cationic Halides, Sequestration of Carbon Dioxide*, Perma-Carb Pty Ltd., Australia, 2007 (Application: WO, 66 pp.).
- [6] L. Marini, *Geological Sequestration of Carbon Dioxide: Thermodynamics, Kinetics, and Reaction Path Modeling*, Elsevier, 2007.
- [7] P.P. Smolin, T.A. Ziborova, *Doklady Akademii Nauk SSSR* 226 (1976) 923–926 (Mineral).
- [8] G.O. Nechiporenko, G.V. Sokolova, T.A. Ziborova, G.P. Bondarenko, *Mineralogicheskii Zhurnal* 10 (1988) 78–85.
- [9] J.H. Canterford, G. Tsambourakis, B. Lambert, *Mineral. Mag.* 48 (1984) 437–442.
- [10] P.J. Davies, B. Bubela, *Chem. Geol.* 12 (1973) 289–300.
- [11] G. Raade, *Am. Mineral.* 55 (1970) 1457–1465.
- [12] H.G.M. Edwards, S.E.J. Villar, J. Jehlicka, T. Munshi, *Spectrochim. Acta A: Mol. Biomol. Spectrosc.* 61A (2005) 2273–2280.
- [13] E. Konigsberger, L.-C. Konigsberger, H. Gamsjager, *Geochim. Cosmochim. Acta* 63 (1999) 3015–3119.
- [14] M. Akao, S. Iwai, *Acta Crystallogr., Sec. B: Struct. Crystallogr. Crystal Chem.* B33 (1977) 3951–3953.
- [15] J.R. Guenter, H.R. Oswald, *J. Solid State Chem.* 21 (1977) 211–215.
- [16] K.N. Goswami, *Indian J. Pure Appl. Phys.* 12 (1974) 667–669.
- [17] H. Jagodzinski, *Mineral. Petrog. Mitt.* 10 (1965) 297–330.
- [18] M. deWolff, *Acta Cryst.* 5 (1952) 286–287.
- [19] M. Fenoglio, *Periodico di Mineralogia* 13 (1942) 1–10.
- [20] L. Brugnatelli, *Centr. Min.* 35 (1903) 144–148.
- [21] L. Brugnatelli, *Rend. Ist. Lombardo* 35 (1902) 869–874.
- [22] S. Caillere, *Compt. Rend.* 219 (1944) 256–258.
- [23] H. Delnavaz, R. Allmann, *Zeitschrift fuer Kristallographie* 183 (1988) 175–178.
- [24] C. Frondel, *Am. Mineral.* 26 (1941) 295–315.
- [25] O.K. Ivanov, *Materialy po Mineral. Mestorozhd, Urala, Sverdlovsk*, 1984, pp. 75–78.
- [26] J.L. Jambor, *Am. Mineral.* 54 (1969) 437–447.
- [27] H. Kolmer, W. Postl, *Mitteilungsblatt - Abteilung fuer Mineralogie am Landesmuseum Joanneum* 45 (1977) 137–141.
- [28] F.A. Mumpton, H.W. Jaffe, C.S. Thompson, *Am. Mineral.* 50 (1965) 1893–1913.

- [29] J. Pastor-Rodriguez, H.F.W. Taylor, *Mineral. Mag. J. Mineral. Soc.* (1876–1968) 38 (1971) 286–294.
- [30] E. Artini, *Atti della Accademia Nazionale dei Lincei, Classe di Scienze Fisiche, Matematiche e Naturali, Rendiconti* 18 (1910) 3–6.
- [31] S. Caillere, *Bull. Soc. Franc. Mineral.* 66 (1943) 494–502.
- [32] M. Fenoglio, *Rev. Geol.* 19 (1938) 128.
- [33] I.E. Grey, R. Ragozzini, *J. Solid State Chem.* 94 (1991) 244–253.
- [34] H.F.W. Taylor, *Mineral. Mag. J. Mineral. Soc.* (1876–1968) 37 (1969) 338–342.
- [35] R.L. Frost, A.W. Musumeci, M.O. Adebajo, W. Martens, *J. Therm. Anal. Calorim.* 89 (2007) 95–99.
- [36] A. Botha, C.A. Strydom, *Hydrometallurgy* 62 (2001) 175–183.
- [37] R.L. Frost, K.L. Erickson, *J. Therm. Anal. Calorim.* 76 (2004) 217–225.
- [38] E. Horvath, J. Kristof, R.L. Frost, N. Heider, V. Vagvolgyi, *J. Therm. Anal. Calorim.* 78 (2004) 687–695.
- [39] R.L. Frost, M.L. Weier, K.L. Erickson, *J. Therm. Anal. Calorim.* 76 (2004) 1025–1033.
- [40] R.L. Frost, K.L. Erickson, *J. Therm. Anal. Calorim.* 78 (2004) 367–373.
- [41] E. Horvath, J. Kristof, R.L. Frost, A. Redey, V. Vagvolgyi, T. Cseh, *J. Therm. Anal. Calorim.* 71 (2003) 707–714.
- [42] J. Kristof, R.L. Frost, J.T. Kloprogge, E. Horvath, E. Mako, *J. Therm. Anal. Calorim.* 69 (2002) 77–83.
- [43] R.L. Frost, W. Martens, Z. Ding, J.T. Kloprogge, *J. Therm. Anal. Calorim.* 71 (2003) 429–438.
- [44] H.C. Helgeson, J.M. Delany, H.W. Nesbitt, D.K. Bird, *Summary and Critique of the Thermodynamic Properties of Rock-forming Minerals, Mineralogical and Geological Chemistry, USA*, 1978.
- [45] J.M. Delany, H.C. Helgeson, *Am. J. Sci.* 278 (1978) 638–686.
- [46] C.W. Beck, *Am. Mineral.* 35 (1950) 985–1013.
- [47] R.A. Robie, B.S. Hemingway, *Thermodynamic properties of minerals and related substances at 298.15 K and 1 Bar (105 Pascals) pressure and at higher temperatures*, U. S. Geol. Survey Bull. (1995), 2131.